

The authors congratulate Academician I.L. Eremenko with a 70th birthday

## Synthesis and Spin State of the Iron(II) Complex with the $N,N'$ -Disubstituted 2,6-Bis(pyrazol-3-yl)pyridine Ligand

I. A. Nikovskii<sup>a</sup>, A. V. Polezhaev<sup>a, b</sup>, D. Yu. Aleshin<sup>a, c</sup>, E. K. Mel'nikova<sup>a, d</sup>, and Yu. V. Nelyubina<sup>a, e, \*</sup>

<sup>a</sup>Nesmeyanov Institute of Organoelement Compounds, Russian Academy of Sciences, Moscow, 119991 Russia

<sup>b</sup>Bauman State Technical University, Moscow, 107005 Russia

<sup>c</sup>Mendeleev University of Chemical Technology of Russia, Moscow, 125047 Russia

<sup>d</sup>Moscow State University, Moscow, 119899 Russia

<sup>e</sup>Kurnakov Institute of General and Inorganic Chemistry, Russian Academy of Sciences, Moscow, 119991 Russia

\*e-mail: unelya@ineos.ac.ru

Received December 7, 2019; revised January 27, 2020; accepted January 31, 2020

**Abstract**—The reaction of a new tridentate ligand 2,6-bis(5-*tert*-butyl-1-(2,6-difluorophenyl)-1*H*-pyrazol-3-yl)pyridine (L) with the divalent iron salt affords the iron(II) complex [Fe(L)<sub>2</sub>](BF<sub>4</sub>)<sub>2</sub> (I), which is isolated in the individual state and characterized by elemental analysis, NMR spectroscopy, and X-ray diffraction analysis. According to the X-ray diffraction results and data of the Evans method, which makes it possible to determine the spin state of paramagnetic compounds in a solution from the NMR spectra, the iron(II) ion in complex I exists in the high-spin state ( $S = 2$  for Fe(II)) and undergoes no temperature-induced spin transition in a range of 120–345 K.

**Keywords:** bis(pyrazolyl)pyridines, cobalt complexes, Evans method, X-ray diffraction analysis, spin state, NMR spectroscopy

**DOI:** 10.1134/S107032842006007X

### INTRODUCTION

Some transition metal complexes can exist in two spin states and can be switched between them under an appropriate external stimulus [1], such as a change in the temperature and pressure, light irradiation, or magnetic field application. A similar spin transition results in a change in various physical properties, including the magnetic moment [1], color [2], dielectric constant [3], and electrical resistance [4]. This makes it possible to use the corresponding transition metal complexes for the production of diverse molecular devices and materials, including displays, the color of which is switched using point heating and cooling [5], films in electroluminescence devices in which the light radiation is quenched due to a change in its electrical resistance [6], etc.

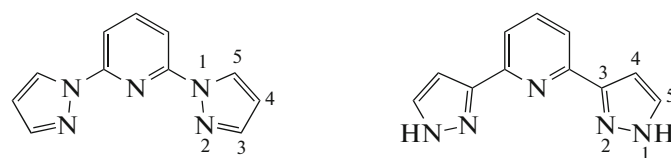
Among a large variety of molecular compounds capable of undergoing the spin transition primarily under the action of temperature [1], this ability is most often found in the iron(II) complexes with the

metal ion in the (pseudo)octahedral environment of the nitrogen-containing heterocyclic ligands [1]. The introduction into the corresponding ligands of substituents of different nature, providing the ligand field necessary for the spin transition, and capable of forming strong intermolecular interactions (hydrogen bonds, stacking interactions, etc.), which result in a sharp spin transition with the hysteresis in the crystalline sample [1], and a systematic analysis of the influence of these modifications of the ligand on the spin state of the metal ion [7–16] form a basis for the targeted “molecular” design [17] of metal complexes with specified parameters of the spin transition.

2,6-Bis(pyrazol-1-yl)pyridines [18] and isomeric 2,6-bis(pyrazol-3-yl)pyridines [19] are among the most popular classes of ligands for this purpose [17] due to the broadest possibilities of their chemical functionalization [19] (Scheme 1). In particular, this made it possible to observe the dependence of the spin state of the iron(II) ion in the metal complexes with

2,6-bis(pyrazol-1-yl)pyridines containing substituents in different positions of the pyridine and pyrazol-1-yl fragments on the steric [17] and electronic [10]

characteristics of these substituents, which allow one to control the spin transition and its parameters, first of all, temperature.



2,6-Bis(pyrazol-1-yl)pyridine

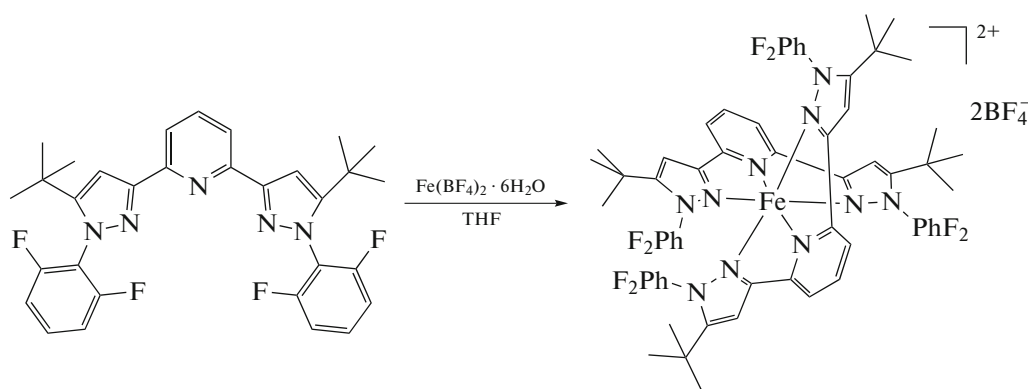
2,6-Bis(pyrazol-3-yl)pyridine

Scheme 1.

Unfortunately, no similar relationships were observed so far for the complexes with isomeric 2,6-bis(pyrazol-3-yl)pyridines [17] because of the N–H...X hydrogen bonds that they form with counterions or solvent molecules (Scheme 1), which unpredictably affect the spin state of the metal ion [20–24]. The single solution of the problem is the search for an appropriate substituent, the introduction of which into position 1 of the pyrazol-3-yl ring does not impede the spin transition to occur, as observed for all presently known iron(II) complexes with 2,6-bis(pyrazol-3-yl)pyridine, 2,6-bis(pyrazol-1-yl)pyridine, and other tridentate nitrogen-containing ligands [17] due to the stabilization of the high-spin state of the metal ion by the bulky substituents near the coordinating nitrogen atoms.

We have previously synthesized a series of the iron(II) bis(pyrazol-3-yl)pyridine complexes with the

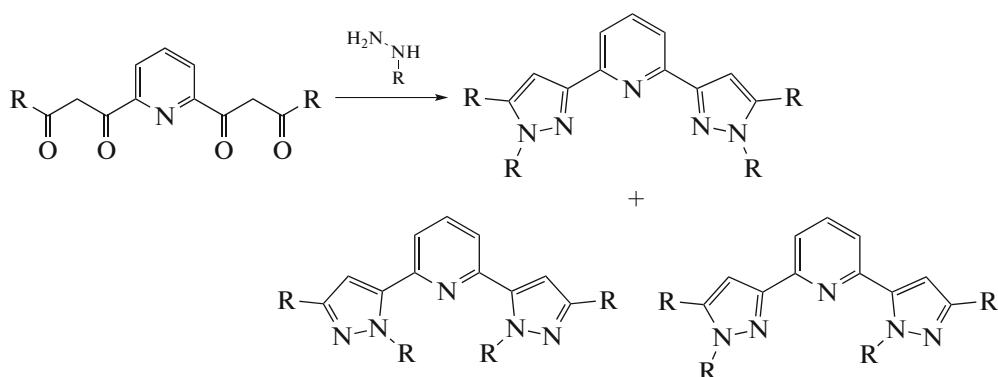
substituted phenyl groups in position 1 of the pyrazol-3-yl ring. Owing to the steric influence of the substituents in the *ortho* position of the phenyl groups, these complexes make it possible to observe the temperature-induced spin transition [25] when choosing alkyl groups and halogen atoms, except for fluorine, as the corresponding substituents. In this case, for the potential appearance of the spin transition, we synthesized a new 2,6-bis(pyrazol-3-yl)pyridine ligand containing the difluorophenyl group in position 1 of the pyrazol-3-yl ring and the electron-donating and bulky *tert*-butyl group in position 5 of the pyrazol-3-yl ring (Scheme 2). A similar modification of position 4 of the pyrazol-1-yl ring of 2,6-bis(pyrazol-3-yl)pyridine earlier led to the stabilization of the low-spin state of the iron(II) ion in the corresponding complexes [10, 17].



Scheme 2.

The introduction of sterically hindered substituents simultaneously into positions 1 and 5 of the pyrazol-3-yl ring of the 2,6-bis(pyrazol-3-yl)pyridine ligands

was not previously performed in connection with the possibility of forming a mixture of the regioisomers (Scheme 3) by the standard synthetic approach [26].



Scheme 3.

In this work, we synthesized the necessary 5-*tert*-butyl-1-phenyl-substituted derivative of 2,6-bis(pyrazol-3-yl)pyridine, 2,6-bis(5-*tert*-butyl-1-(2,6-difluorophenyl)-1*H*-pyrazol-3-yl)pyridine (L), and its complex [Fe(L)<sub>2</sub>](BF<sub>4</sub>)<sub>2</sub> (I) in high yields. The spin state of the iron(II) ion in the complex, whose *N,N'*-disubstituted ligand contains the *tert*-butyl group in position 5 of the pyrazol-3-yl ring, was determined by X-ray diffraction analysis of the single crystal at 120 K. The possibility of the spin transition to occur in a solution of complex I with temperature effect was studied using the Evans method, which is standard for these purposes [27] and based on multitemperature NMR spectroscopy.

## EXPERIMENTAL

All procedures related to the synthesis of the bis(pyrazol-3-yl)pyridine ligand and its complex were carried out in air using commercially available organic solvents distilled in an argon atmosphere. Iron tetrafluoroborate hexahydrate Fe(BF<sub>4</sub>)<sub>2</sub> · 6H<sub>2</sub>O (Sigma-Aldrich) was used without additional purification. The esterification of pyridine-2,6-dicarboxylic acid (Acros) with ethanol was carried out using a described procedure [28] in the presence of sulfuric acid. Analyses to carbon, nitrogen, and hydrogen were conducted on a CarloErba microanalyzer (model 1106).

**Synthesis of 1,1'-(pyridine-2,6-diyl)bis(4,4-dimethylpentane-1,3-dione).** A solution of diethyl pyridine-2,6-dicarboxylate (2.80 g, 12.5 mmol) in anhydrous THF was mixed with NaH (1.22 g, 30.5 mmol, 50% suspension of mineral oil). *tert*-Butyl methyl ketone (3.40 mL, 27.5 mmol) was added dropwise to the obtained suspension. The reaction mixture was refluxed with a reflux condenser for 4 h and evaporated. The solid residue was washed with diethyl ether (2 × 30 mL), dried in vacuo, and dispersed in water, and the pH of the resulting suspension was brought to pH 5 by adding 1 M hydrochloric acid. A dark yellow precipitate was filtered off, dried in vacuo, dissolved in a minor amount of hot ethanol, and left at -20°C for

12 h. The formed yellow crystals were separated by filtration and dried in vacuo. The yield was 2.87 g (69%).

<sup>1</sup>H NMR (CDCl<sub>3</sub>, 400 MHz), δ, ppm: 16.12, 15.89 (s, OH), 8.26–8.17 (m, *m*-Py-H, 2H), 8.01–7.96 (m, *p*-Py-H, 1H), 7.21, 6.91, and 4.51 (s, CH and CH<sub>2</sub>), 1.29, 1.27, and 1.25 (s, <sup>t</sup>Bu, 18H). <sup>13</sup>C NMR (100 MHz, CDCl<sub>3</sub>, mixture of keto and enol forms), δ, ppm: 210.4, 204.6, and 203.0 (CH), 196.5 and 182.5 (CH-COH), 181.0, 152.5, 152.1, and 152.0 (*o*-Py), 138.4 (*p*-Py), 125.6, 124.3, and 124.1 (*m*-Py), 92.9 and 92.8 (CH), 46.4 (CH<sub>2</sub>), 45.1, 40.4, and 40.0 (<sup>t</sup>Bu), 27.4 and 26.7 (<sup>t</sup>Bu).

For C<sub>19</sub>H<sub>25</sub>NO<sub>4</sub>

Anal. calcd., %:	C, 68.86	H, 7.60	N, 4.23
Found, %:	C, 68.79	H, 7.66	N, 4.18

**Synthesis of 2,6-difluorophenylhydrazine.** 2,6-Difluoroaniline (3.87 g, 30.0 mmol) was added to a 38% aqueous solution of HCl (25 mL). A solution of sodium nitrite (2.17 g, 31.5 mmol) in water (5 mL) was added dropwise to the obtained suspension preliminarily cooled to -10°C maintaining the temperature below -5°C. The reaction mixture was stirred at -10°C for 1 h. Then a solution of SnCl<sub>2</sub> · 2H<sub>2</sub>O (16.85 g, 75 mmol) in concentrated hydrochloric acid (30 mL) was added dropwise to the resulting mixture at -5°C. The obtained suspension was stirred at room temperature for 1 h, and the precipitate was filtered off and washed with dichloromethane (100 mL). The formed yellow powder was dried in vacuo. The reaction product was stored in the form of the salt, which prior to use was transformed into the free base using a 1 M solution of sodium hydroxide in water. The yield was 3.30 g (61%).

<sup>1</sup>H NMR (CDCl<sub>3</sub>, 300 MHz), δ, ppm: 6.78–6.68 (m, 3H, *m*-Ph and *p*-Ph), 5.30 (br.s, 1H, NH), 3.93 (br.s, 2H, NH<sub>2</sub>). <sup>13</sup>C NMR (DMSO-d<sub>6</sub>, 101 MHz), δ, ppm: 153.73 (q, <sup>1</sup>J<sub>C,F</sub> = 242.4 Hz, <sup>3</sup>J<sub>C,F</sub> = 6.6 Hz, 2-Ph), 128.52 (t, <sup>2</sup>J<sub>C,F</sub> = 12.7 Hz, 1-Ph), 120.46 (t,

$^4J_{C,F} = 7.2$  Hz, 4-Ph), 111.58 (q,  $^2J_{C,F} = 15.9$  Hz,  $^4J_{C,F} = 7.1$  Hz, 3-Ph).

For  $C_6H_6N_2F_2$

Anal. calcd., %	C, 50.00	H, 4.20	N, 19.44
Found, %	C, 50.11	H, 4.23	N, 19.39

**Synthesis of 2,6-bis(5-*tert*-butyl-1-(2,6-difluorophenyl)-1*H*-pyrazol-3-yl)pyridine (L).** Diethyl 1,1'-(pyridine-2,6-diyl)bis(4,4-dimethylpentane-1,3-dione) (1 g, 3.02 mmol) and 2,6-difluorophenyldiazine (1 g, 6.94 mmol) were dissolved in glacial acetic acid (10 mL), and the mixture was refluxed with a reflux condenser for 8 h. The reaction mixture was cooled by adding crushed ice (50 mL). The white precipitate was filtered off, washed with water, and dried in vacuo. For purification, the obtained product was dissolved in hot ethyl acetate, and hexane was added until a precipitate was formed. Then the mixture was kept at  $-10^\circ\text{C}$  for 12 h. The formed white crystals were filtered off and dried in vacuo. The yield was 546 mg (33%).

$^1\text{H}$  NMR ( $\text{CDCl}_3$ , 400 MHz),  $\delta$ , ppm: 1.28 (s, 18H, *t*Bu), 7.06–7.09 (m, 6H, *m*-Ph–H+ Pyraz–CH), 7.44–7.51 (m, 2H, *p*-Ph–H), 7.70 (t,  $^3J_{H,H} = 7.7$  Hz, 1H, Py), 7.90 (d,  $^3J_{H,H} = 7.7$  Hz, 2H, Py).  $^{13}\text{C}$  NMR ( $\text{DMSO-d}_6$ , 101 MHz),  $\delta$ , ppm: 159.52 (q,  $^1J_{C,F} = 254.92$  Hz,  $^4J_{C,F} = 3.3$  Hz, 2-Ph), 156.06 (s, 5-Pyraz), 152.75 (s, 2-Py), 151.53 (s, 3-Pyraz), 136.99 (s, 4-Py), 131.28 (t,  $^3J_{C,F} = 9.9$  Hz, 4-Ph), 119.39 (s, 3-Py), 112.16–112.21 (m, 1-Ph), 111.98–112.02 (m, 3-Ph), 103.49 (s, 4-Pyraz), 29.54 (s, 18H, *t*Bu).  $^{19}\text{F}$  NMR ( $\text{DMSO-d}_6$ , 376 MHz),  $\delta$ , ppm: –115.59 (s, 4F, PhF<sub>2</sub>).

For  $C_{31}H_{29}N_5F_4$

Anal. calcd., %	C, 67.99	H, 5.34	N, 12.79
Found, %	C, 68.21	H, 5.41	N, 12.93

**Synthesis of complex I.** Weighed samples of  $\text{Fe}(\text{BF}_4)_2 \cdot 6\text{H}_2\text{O}$  (0.0337 g, 0.1 mmol) and L (0.109 g, 0.2 mmol) were stirred in THF for 3 h. For purification, the obtained solution was concentrated, and hexane was added dropwise to precipitation. The mixture was kept at  $-10^\circ\text{C}$  for 12 h. The precipitate was filtered off and dried in vacuo. The yield was 226 mg (86%).

$^1\text{H}$  NMR ( $\text{CD}_3\text{CN}$ , 600 MHz),  $\delta$ , ppm: 0.61 (br.s, 36H, *t*Bu), 9.47 (br.s, 8H, *m*-Ph–H), 13.24 (br.s, 4H, *p*-Ph–H), 24.15 (br.s, 2H, *p*-Py–H), 54.78 (br.s, 4H, Pyraz–CH), 63.03 (br.s, 4H, *m*-Py–H).

For  $C_{62}H_{58}B_2N_{10}F_{16}\text{Fe}$

Anal. calcd., %	C, 56.22	H, 4.41	N, 10.57
Found, %	C, 56.02	H, 4.31	N, 10.64

$^1\text{H}$ ,  $^{19}\text{F}$ , and  $^{13}\text{C}$  NMR spectra were recorded in  $\text{DMSO-d}_6$ ,  $\text{CDCl}_3$ , and  $\text{CD}_3\text{CN}$  on Bruker Avance 300, Bruker Avance 400, and Bruker Avance 600 spectrometers (with the working frequencies for protons 300.15, 400, and 600.22 MHz, respectively). The chemical shifts in the spectra were determined relative to the residual signal from the solvent ( $^1\text{H}$  7.26 and  $^{13}\text{C}$  77.16 ppm for  $\text{CDCl}_3$ ,  $^1\text{H}$  2.5 and  $^{13}\text{C}$  39.52 ppm for  $\text{DMSO-d}_6$ , and  $^1\text{H}$  1.94 ppm for  $\text{CD}_3\text{CN}$ ). The spectra were collected using the following parameters. For  $^1\text{H}$  NMR, the spectral range was 1000 ppm, the detection time was 0.1 s, the relaxation delay was 0.1 s, the pulse duration was 6.5  $\mu\text{s}$ , and the acquisition number was 1024. For  $^{13}\text{C}\{^1\text{H}\}$  NMR, the spectral range was 3000 ppm, the detection time was 0.1 s, the relaxation delay was 0.1 s, the pulse duration was 9  $\mu\text{s}$ , and the acquisition number was more than 32000. In the case where the signal to noise ratio was necessary to be increased, the obtained free induction descends were processed by exponential weighing with the coefficient to 3 and 50 Hz for  $^1\text{H}$  and  $^{13}\text{C}$  NMR spectra, respectively.

**X-ray diffraction analysis (XRD).** Single crystals of complex I obtained by the slow evaporation in air from a solution in THF were examined on a Bruker APEX 2 CCD diffractometer ( $\text{MoK}\alpha$  radiation, graphite monochromator,  $\omega$  scan mode). The structure was solved using the ShelXT program [29] and refined by full-matrix least squares using the Olex2 program [30]

in the anisotropic approximation for  $F_{hkl}^2$ . The positions of the hydrogen atoms were calculated geometrically and refined in the isotropic approximation by the riding model. Selected crystallographic data and structure refined parameters are presented in Table 1.

The structural data for complex I were deposited with the Cambridge Crystallographic Data Centre (CIF file CCDC no. 1968406; <http://www.ccdc.cam.ac.uk/>).

**Evans method.** The temperature dependence of the magnetic susceptibility of the iron(II) complex in an acetonitrile solution was estimated by the Evans method [27] in a range of 235–345 K using NMR tubes with a coaxial inset. The inner (control) tube was filled with acetonitrile- $d_3$  with an additive of  $\sim 1\%$   $\text{Me}_4\text{Si}$ , and the outer tube contained a solution of the complex ( $\sim 1\text{--}5$  mg/ $\text{cm}^3$ ) in acetonitrile- $d_3$  with the same concentration of  $\text{Me}_4\text{Si}$ . The molar magnetic susceptibility ( $\chi_M$ ) was calculated from the difference between the chemical shift of  $\text{Me}_4\text{Si}$  in pure acetonitrile- $d_3$  and its shift in a solution of the complex ( $\Delta\delta$ , Hz) in acetonitrile- $d_3$  using the following equation:

$$\chi_M = \frac{\Delta\delta M}{\nu_0 S_f c} - \chi_M^{\text{dia}}$$

( $M$  is the molar weight of the iron(II) complex, g/mol;  $\nu_0$  is the spectrometer frequency, Hz;  $S_f$  is the magnet

**Table 1.** Selected crystallographic data and structure refinement parameters for compound I

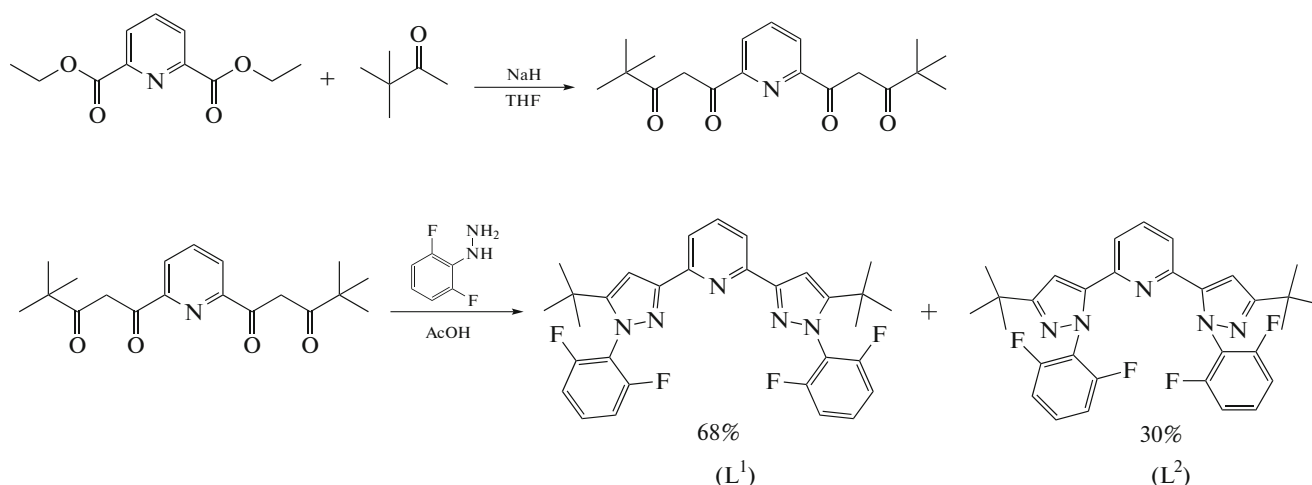
Parameter	Value
<i>FW</i>	1324.65
<i>T</i> , K	120
Crystal system	Monoclinic
Space group	<i>P2<sub>1</sub>/n</i>
<i>Z</i>	4
<i>a</i> , Å	16.062(3)
<i>b</i> , Å	21.690(5)
<i>c</i> , Å	17.244(4)
$\beta$ , deg	90.483(5)
<i>V</i> , Å <sup>3</sup>	6007(2)
$\rho_{\text{calc}}$ , g cm <sup>-3</sup>	1.465
$\mu$ , cm <sup>-1</sup>	3.51
<i>F</i> (000)	2720
$2\theta_{\text{max}}$ , deg	60
Number of measured reflections	82175
Number of independent reflections ( <i>R</i> <sub>int</sub> )	18365 (0.0769)
Number of reflections with <i>I</i> > 3 $\sigma$ ( <i>I</i> )	12297
Number of refined parameters	851
GOOF	1.010
<i>R</i> <sub>1</sub> , <i>wR</i> <sub>2</sub> ( <i>I</i> > 2 $\sigma$ ( <i>I</i> ))	0.0478, 0.1014
<i>R</i> <sub>1</sub> , <i>wR</i> <sub>2</sub> (all data)	0.0869, 0.1181
$\Delta\rho_{\text{max}}/\Delta\rho_{\text{min}}$ , e Å <sup>-3</sup>	0.398/−0.346

shape coefficient ( $4\pi/3$ ); *c* is the concentration of the complex, g/cm<sup>3</sup>; and  $\chi_{\text{M}}^{\text{dia}}$  is the molar diamagnetic contribution to the paramagnetic susceptibility calculated using Pascal's constants [31]). The concentration *c* was recalculated for each temperature according to a change in the solvent density ( $\rho$ ):  $c_{\text{T}} = m_{\text{c}}\rho/m_{\text{sol}}$ , where  $m_{\text{c}}\rho$  is the weight of the complex, and  $m_{\text{sol}}$  is the weight of the solution.

## RESULTS AND DISCUSSION

For the synthesis of ligand L, the initial 1,1'-(pyridine-2,6-diyl)bis(4,4-dimethylpentane-1,3-dione) was

synthesized using a described procedure [32] by the Claisen condensation between diethyl-2,6-pyridinedicarboxylate and pinacone in the presence of sodium hydride in a THF solution. The condensation of the obtained diketone and 2,6-difluorophenylhydrazide followed by cyclization in one step in acetic acid resulted in a mixture of regioisomers with the predomination of the required bis(pyrazol-3-yl)pyridine L (L<sup>1</sup> in Scheme 4). Owing to different solubilities of two regioisomers, this product is readily isolated in the pure state by the recrystallization of the mixture in an ethyl acetate–hexane (1 : 1) system. Interestingly, nearly no mixed regioisomer was formed in this synthetic approach (Scheme 3).



Scheme 4.

The reaction of bis(pyrazol-3-yl)pyridine L with iron(II) tetrafluoroborate hydrate in THF at room temperature (Scheme 3) was carried out for the synthesis of the corresponding iron(II) complex I. The complex was isolated in the individual state and characterized by elemental analysis, NMR spectroscopy, and XRD.

In spite of the electron-donating substituent in position 5 of the pyrazol-3-yl ring in ligand L, which resulted in the stabilization of the low-spin state of the iron(II) ion in the case of the complexes with isomeric bis(pyrazol-3-yl)pyridines, crystalline complex I exists in the high-spin state according to the XRD data at 120 K. This is indicated by the Fe–N distances with the nitrogen atoms of two bis(pyrazol-3-yl)pyridine ligands (Table 2) typical of the high-spin iron(II) complexes with the nitrogen-containing heterocycles (2.0–2.2 Å [1]). In addition, the coordination polyhedron FeN<sub>6</sub>, which is an octahedron in the low-spin

state, is distorted toward a trigonal prism [33]. The corresponding angles N(Py)MN(Py) and  $\theta$  between the root-mean-square planes of two ligands, which are equal to 90° and 180° in the case of an ideal octahedron, are 86.802(15)° and 176.80(6)°, respectively. For comparison, similar values for the earlier described iron(II) complexes [34] with *N,N'*-diphenyl-substituted bis(pyrazole-3-yl)pyridines lie in the ranges 67.5(3)°–68.3(3)° and 176.1(2)°–180°, respectively.

A less pronounced deviation of the coordination polyhedron shape in complex I from an octahedron is caused, most likely, by the presence of the bulky *ortho*-difluorophenyl groups in position 1 of the pyrazol-3-yl cycle, which rotate relative to the plane of this cycle due to the steric effects of the *ortho* substituents (Fig. 1), stabilizing the (pseudo)octahedral molecular geometry of complex I. In fact, the rotation angles of the *ortho*-substituted phenyl groups in it are 85.56(7)°–88.82(7)°, which appreciably exceeds similar values (42.7(2)°–66.4(2)°) in the iron(II) complexes with the *N,N'*-diphenyl-substituted bis(pyrazol-3-yl)pyridine ligands [34].

Nevertheless, this does not result in the absence in complex I of the trigonal prismatic distortion of the coordination polyhedron characteristic of the high-spin iron(II) complexes with the bi- and tridentate ligands [35]. This can graphically be presented as the so-called “continuous symmetry measures” [35] describing deviations of the shape of the coordination polyhedron FeN<sub>6</sub> from an ideal octahedron (S(OC-6)) and an ideal trigonal prism (S(TP-6)). The lower these values, the better the description of the coordination polyhedron shape by the corresponding polyhedron (Fig. 2). In complex I, the octahedral S(OC-6) and trigonal prismatic S(TP-6) “continuous symmetry measures” estimated from the XRD data using the Shape 2.1 program [35] are 5.460 and 10.780, respectively (Table 2). They fall onto the range of the “continuous symmetry measures” S(OC-6) and S(TP-6) for the high-spin iron(II) complexes [34] with *N,N'*-

**Table 2.** Selected geometric parameters for complex I according to the XRD data at 120 K\*

Parameter	Value
M–N(Py), Å	2.1507(14)/2.1527(15)
M–N(Pz), Å	2.1749(15)–2.2043(15)
$\theta$ , deg	86.802(15)
N(Py)MN(Py), deg	176.80(6)
$\alpha$ , deg	85.56(7)–88.82(7)
S(TP-6)	10.780
S(OC-6)	5.460

\*  $\theta$  is the dihedral angle between the root-mean-square planes of the 2,6-bis(pyrazol-3-yl)pyridine ligands, the N(Py) and N(Pz) atoms correspond to the nitrogen atoms of the pyridine and pyrazol-3-yl fragments, and  $\alpha$  corresponds to the rotation angle of the difluorophenyl substituents relative to the plane of the pyrazol-3-yl ring. S(TP-6) and S(OC-6) are the deviations of the MN<sub>6</sub> coordination polyhedron from an ideal trigonal prism (TP-6) and an ideal octahedron (OC-6), respectively.

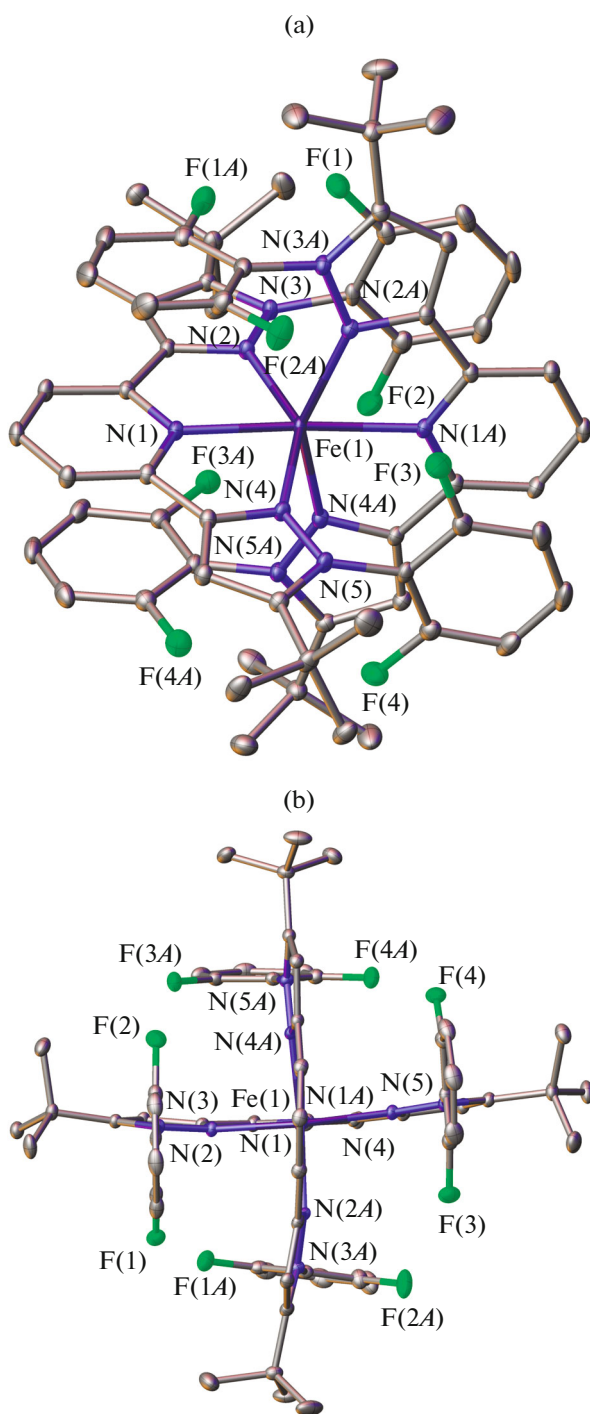


**Fig. 1.** (a) General view of complex I and (b) its projection in the perpendicular direction in atomic representation by thermal ellipsoids ( $p = 50\%$ ). Tetrafluoroborate anions and hydrogen atoms are omitted, and only heteroatoms are labeled.

diphenyl-substituted bis(pyrazol-3-yl)pyridines in which the coordination environment of the metal ion is noticeably distorted toward a trigonal prism, which does not allow it to transform into the low-spin state [36].

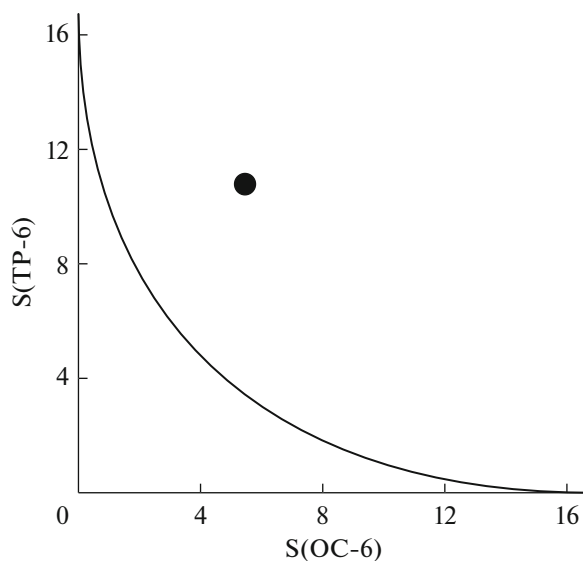


**Fig. 2.** Graphical representation of the “continuous symmetry measures”  $S(\text{TP-6})$  and  $S(\text{OC-6})$  describing the deviation of the  $\text{FeN}_6$  polyhedron in the crystal of compound I ( $\bullet$ ) from an ideal trigonal prism (TP-6) and an ideal octahedron (OC-6), respectively. Black line shows the route of the least distortion of the polyhedron geometry on going between the indicated polyhedra.

Thus, the XRD data for complex I indicate that the iron(II) ion exists in the high-spin state in the crystal at 120 K in the environment of two bis(pyrazol-3-yl)pyridine ligands L with the bulky difluorophenyl substituents in position 1 of the pyrazol-3-yl ring [17].

Complex I exists in the same spin state in a range of 235–345 K in an acetonitrile solution, which is unambiguously confirmed by the Evans method [27], which is based on the use of NMR spectroscopy. This method is the most available one for measuring  $\chi_M$  of a solution, because of which the Evans method is actively used for the search for structure–property relationships in the absence of crystalline packing effects often leading to blocking the metal ion in one spin state [36] and for the consecutive targeted design of metal complexes with specified parameters of the spin transition [17]. To measure  $\chi_M$  of a solution varying upon the addition of a paramagnetic compound, such as the iron(II) complex in the high-spin state (see Experimental), the NMR spectra of a solution of a standard compound (usually tetramethylsilane (TMS)) in the presence and in the absence of a paramagnetic complex are simultaneously collected in the Evans method. For this purpose, a standard tube containing a solution of the corresponding complex and TMS in a known concentration is inserted with a special coaxial inset containing a TMS solution in the same solvent in which no precipitate would be formed on cooling, which is one of restraints of the Evans method. The difference between the chemical shifts of TMS in the NMR spectra collected from these two

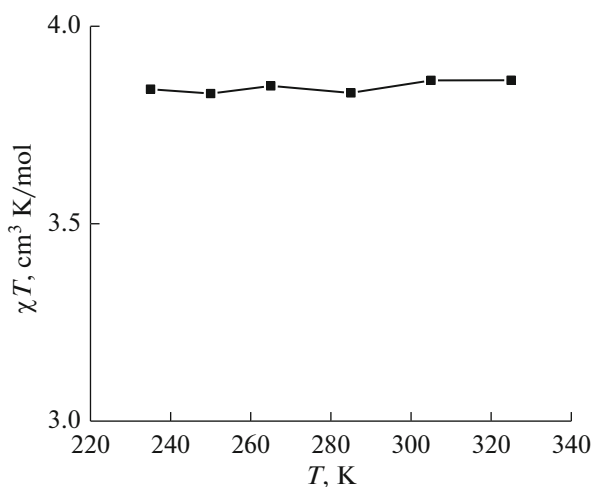


**Fig. 3.** Temperature dependence of the magnetic susceptibility of complex **I** in a solution of deuterated acetonitrile according to the NMR spectroscopy data (Evans method).

solutions makes it possible to calculate  $\chi_M$  of a solution of the studied paramagnetic compound and thus unambiguously determine the spin state of the metal ion at a certain temperature or in the range of temperatures accessible for the chosen solvent.

According to thus obtained data, the values of  $\chi T$  for a solution of complex **I** in an acetonitrile at temperatures in a range of 235–345 K (Fig. 3) are close to  $3.8 \text{ cm}^3 \text{ mol}^{-1} \text{ K}$ , which unambiguously confirms the high-spin state of the iron(II) ion ( $S = 2$ ) in the whole temperature range. The observed stabilization of the high-spin state in the solution in which the crystal packing effects are absent indicates in favor of the “intramolecular” nature of this phenomenon caused, most likely, by the presence in the ligand of the bulky *ortho*-substituted phenyl groups near the coordinating nitrogen atoms [17]. In turn, this indicates an insufficient electronic and steric influence of the *tert*-butyl substituents in position 5 of the pyrazol-3-yl ring leading, as a result, to the absence of the temperature-induced spin transition in complex **I**.

To conclude, we synthesized and characterized the new iron(II) complex with the *N,N'*-substituted 2,6-bis(pyrazol-3-yl)pyridine ligand containing the bulky substituents simultaneously in positions 1 and 5 of the pyrazol-3-yl ring. The low-temperature XRD data obtained for this complex, first of all, the M–N bond lengths and the trigonal prismatic distortion of the coordination polyhedron of the iron(II) ion, unambiguously indicate that the complex exists in the high-spin state ( $S = 2$ ) in the crystal even at 120 K. The absence of the temperature-induced spin transition in the solution in a range of 235–345 K is confirmed by NMR spectroscopy (Evans method). Thus, the introduction of the electron-donating and sterically hindered substituent (*tert*-butyl group) into position 5 of the pyrazol-3-yl ring of 2,6-bis(pyrazol-3-yl)pyridine

containing a bulky *N*-substituent exerts no effect on the spin state of the iron(II) ion in the corresponding complex, which remains high-spin in both the crystalline state and acetonitrile solution.

#### FUNDING

The XRD studies of the metal complexes were collected with a support from the Ministry of Science and Higher Education of the Russian Federation using the scientific equipment of the Center of Molecular Structure Investigation at the Nesmeyanov Institute of Organoelement Compounds (Russian Academy of Sciences).

This work was supported by the Russian Science Foundation, project no. 17-13-01456.

#### CONFLICT OF INTEREST

The authors declare that they have no conflicts of interest.

#### REFERENCES

1. *Spin-Crossover Materials: Properties and Applications*, Halcrow M.A., Ed., New York: Wiley, 2013.
2. König, E., *Progress in Inorganic Chemistry*, 2007, p. 527.
3. Bousseksou, A., Molnár, G., Demont, P., and Mene-gotto, J., *J. Mat. Chem.*, 2003, vol. 13, no. 9, p. 2069.
4. Matsuda, M. and Tajima, H., *Chem. Lett.*, 2007, vol. 36, no. 6, p. 700.
5. Kahn, O. and Martinez, C.J., *Science*, 1998, vol. 279, no. 5347, p. 44.
6. Matsuda, M., Isozaki, H., and Tajima, H., *Thin Solid Films*, 2008, vol. 517, no. 4, p. 1465.
7. Phan, H., Hrudka, J.J., Igimbayeva, D., et al., *J. Am. Chem. Soc.*, 2017, vol. 139, no. 18, p. 6437.
8. Rodríguez-Jiménez, S., Yang, M., Stewart, I., et al., *J. Am. Chem. Soc.*, 2017, vol. 139, no. 50, p. 18392.
9. Kimura, A. and Ishida, T., *ACS Omega*, 2018, vol. 3, no. 6, p. 6737.
10. Kershaw Cook, L.J., Kulmaczewski, R., Mohammed, R., et al., *Angew. Chem., Int. Ed. Engl.*, 2016, vol. 55, no. 13, p. 4327.
11. Elhaik, J., Evans, D.J., Kilner, C.A., and Halcrow, M.A., *Dalton Trans.*, 2005, no. 9, p. 1693.
12. McPherson, J.N., Elton, T.E., and Colbran, S.B., *Inorg. Chem.*, 2018, vol. 57, no. 19, p. 12312.
13. Santoro, A., Kershaw Cook, L.J., Kulmaczewski, R., et al., *Inorg. Chem.*, 2015, vol. 54, no. 2, p. 682.
14. Nakano, K., Suemura, N., Yoneda, K., et al., *Dalton Trans.*, 2005, no. 4, p. 740.
15. Kitchen, J.A., Olguin, J., Kulmaczewski, R., et al., *Inorg. Chem.*, 2013, vol. 52, no. 19, p. 11185.
16. Hoselton, M., Wilson, L.J., and Drago, R.S., *J. Am. Chem. Soc.*, 1975, vol. 97, no. 7, p. 1722.
17. Halcrow, M.A., *Crystals*, 2016, vol. 6, no. 5, p. 58.
18. Halcrow, M.A., *Coord. Chem. Rev.*, 2009, vol. 253, no. 21, p. 2493.

19. Halcrow, M.A., *Coord. Chem. Rev.*, 2005, vol. 249, no. 25, p. 2880.
20. Scudder, M.L., Craig, D.C., and Goodwin, H.A., *CrystEngComm*, 2005, vol. 7, no. 107, p. 642.
21. Clemente-León, M., Coronado, E., Giménez-López, M.C., and Romero, F.M., *Inorg. Chem.*, 2007, vol. 46, no. 26, p. 11266.
22. Coronado, E., Giménez-López, M.C., Gimenez-Saiz, C., and Romero, F.M., *CrystEngComm*, 2009, vol. 11, no. 10, p. 2198.
23. Bartual-Murgui, C., Codina, C., Roubeau, O., and Ar-omi, G., *Chem.-Eur. J.*, 2016, vol. 22, no. 36, p. 12767.
24. Jornet-Molla, V., Gimenez-Saiz, C., and Romero, F.M., *Crystals*, 2018, vol. 8, p. 439.
25. Nikovskiy, I., Polezhaev, A., Novikov, V., et al., *Chem.-Eur. J.*, 2020.  
<https://doi.org/10.1002/chem.202000047>
26. van der Valk, P. and Potvin, P.G., *Org. Chem.*, 1994, vol. 59, no. 7, p. 1766.
27. Evans, D.F., *J. Chem. Soc. (Resumed)*, 1959, p. 2003.
28. Polezhaev, A.V., Chen, C.-H., Kinne, A.S., et al., *Inorg. Chem.*, 2017, vol. 56, no. 16, p. 9505.
29. Sheldrick, G.M., *Acta Crystallogr., Sect. A: Found. Crystallogr.*, 2008, vol. 64, p. 112.
30. Dolomanov, O.V., Bourhis, L.J., Gildea, R.J., et al., *J. Appl. Crystallogr.*, 2009, vol. 42, p. 339.
31. Bain, G.A. and Berry, J.F., *J. Chem. Educ.*, 2008, vol. 85, no. 4, p. 532.
32. Korzekwa, J., Scheurer, A., Heinemann, F.W., and Meyer, K., *Dalton Trans.*, 2017, vol. 46, no. 40, p. 13811.
33. Alvarez, S., *J. Am. Chem. Soc.*, 2003, vol. 125, no. 22, p. 6795.
34. Nelyubina, Y.V., Polezhaev, A.V., Pavlov, A.A., et al., *Magnetochemistry*, 2018, vol. 4, no. 4, p. 46.
35. Alvarez, S., *Chem. Rev.*, 2015, vol. 115, p. 13447.
36. Kershaw, Cook, L., Mohammed, R., Sherborne, G., et al., *Coord. Chem. Rev.*, 2015, vols. 289–290, p. 2.

*Translated by E. Yablonskaya*